A computational strategy for multiphysics problems involving nonlinear aspects

David Dureisseix, David Néron, Pierre Ladevèze, Bernard A. Schrefler

European Congress on Computational Methods in Applied Sciences and Engineering
ECCOMAS 2004
P. Neittaanmäki, T. Rossi, S. Korotov, E. Oñate, J. Périaux, and D. Knörzer (eds.)
Jyväskylä, 24–28 July 2004

A COMPUTATIONAL STRATEGY FOR MULTIPHYSICS PROBLEMS INVOLVING NONLINEAR ASPECTS

D. Dureisseix*, D. Néron†, P. Ladevèze† and B. A. Schrefler‡

* LMGC (Montpellier 2 University/CNRS)
CC 048, place Eugène Bataillon, F-34095 Montpellier CEDEX 5, France
dureisse@lmgc.univ-montp2.fr

† LMT-Cachan (ENS Cachan/CNRS/Paris 6 University)
61, avenue du Président Wilson, F-94235 Cachan CEDEX, France
{neron,ladeveze}@lmt.ens-cachan.fr

‡ Department of Structural and Transportation Engineering (University of Padova)
Via Marzolo 9, I-35131 Padova, Italy
bas@caronte.dic.unipd.it

Key words: multiphysics, nonlinear, multiscale, LATIN, porous media

Abstract. *Multiphysics phenomena lead to computationally intensive structural analyses. Recently, a new strategy derived from the LATIN method was described and successfully applied to the consolidation of saturated porous soils.*

One of the main achievements was the use of the LATIN method to take into account the different time scales which usually arise from the different physics: a multi-time-scale strategy was proposed.

We focus herein on two different improvements of the aforementioned approach: (i) we study the behavior of the method for classical nonlinearities involved in poroelasticity problems and (ii) to improve modularity of the partitioning we propose a multi-space-scale appoach to deal with independent meshes for each physics.

1 MULTIPHYSICS COUPLED PROBLEMS

1.1 Introduction

For coupled multiphysics problems such as fluid-structure interaction, partitioned procedures and staggered algorithms are often preferred, from the point of view of computational efficiency, to direct analysis (also called the monolithic approach). Moreover, partitioning strategies enable one to use different analyzers for different subsystems, and help keep the software manageable.

A typical example of a highly coupled fluid-structure interaction problem is the consolidation of saturated porous soils. The term *consolidation* designates the slow deformation of the solid phase accompanied by flow of the pore fluid. One of the consequences of natural consolidation is surface subsidence, i.e. the lowering of the ground surface. The consolidation analysis of soils has long been recognized as an important problem in civil engineering design [1].

1.2 Example of linear poroelacticity

Let us briefly describe a typical consolidation problem [1, 2]. A structure Ω is made of a saturated porous material undergoing small perturbations and isothermal evolution over the time interval $[0,T]$ being studied.

The loading consists of a prescribed displacement $\underline{U}_d$ on a part $\partial_1\Omega$ of the boundary, a traction force $\underline{F}_d$ on the complementary part $\partial_2\Omega$ of $\partial_1\Omega$, a fluid flux w_d on another part $\partial_3\Omega$ of the boundary and, finally, a prescribed pore pressure p_d on the complementary part $\partial_4\Omega$ of $\partial_3\Omega$. For the sake of simplicity, we assume that there are no body forces.

For solid quantities, strain and stress are denoted $\boldsymbol{\varepsilon}$ and $\boldsymbol{\sigma}$ respectively; for fluid quantities, the pore pressure gradient is denoted $\underline{Z}$ and the opposite of Darcy's velocity $\underline{W}$; finally, q denotes the rate of fluid mass accumulation in each representative elementary volume.

The state of the structure is given by the set of the fields $\mathbf{s} = (\boldsymbol{\varepsilon}, p, \underline{Z}, \boldsymbol{\sigma}, q, \underline{W})$ defined on the whole structure Ω and over the time interval $[0,T]$ being considered. The problem consists in finding $\mathbf{s}$ in the corresponding space $\mathbf{S}^{[0,T]}$ which verifies at each time step the following equations:

- in the solid, compatibility of strains $\boldsymbol{\varepsilon}$ and equilibrium of stresses $\boldsymbol{\sigma}$:

$$\begin{aligned} \underline{U} \in \mathcal{U}^{[0,T]} \quad \text{and} \quad \boldsymbol{\varepsilon} = \boldsymbol{\varepsilon}(\underline{U}) \quad \text{on } \Omega \\ \underline{\mathrm{div}}\boldsymbol{\sigma} = \underline{0} \quad \text{on } \Omega \quad \text{and} \quad \boldsymbol{\sigma}\underline{n} = \underline{F}_d \quad \text{on } \partial_2\Omega \end{aligned} \tag{1}$$

  $\mathcal{U}^{[0,T]}$ being the set of the finite-energy displacement fields on $\Omega \times [0,T]$ equal to $\underline{U}_d$ on $\partial_1\Omega$;

- in the fluid, flow conservation for Darcy's velocity $-\underline{W}$:

$$\begin{aligned} p \in \mathcal{P}^{[0,T]} \quad \text{and} \quad \underline{Z} = \underline{\text{grad}}\, p \quad \text{on } \Omega \\ q = \text{div}\, \underline{W} \quad \text{on } \Omega \quad \text{and} \quad \underline{W} \cdot \underline{n} = w_d \quad \text{on } \partial_4\Omega \end{aligned} \tag{2}$$

  $\mathcal{P}^{[0,T]}$ being the set of the finite-energy pressure fields on $\Omega \times [0,T]$ equal to p_d on $\partial_3\Omega$;

- the constitutive relations:
  - Hooke's law, which relates the macroscopic stress $\boldsymbol{\sigma}$ to the strain $\boldsymbol{\varepsilon}$ and the pore pressure p so that:

$$\boldsymbol{\sigma} = \mathbf{D}\boldsymbol{\varepsilon} - bp\mathbf{I} \tag{3}$$

  - Darcy's law, which relates Darcy's velocity to the pore pressure gradient:

$$\underline{W} = \frac{K}{\mu_w}\underline{Z} \tag{4}$$

  - compressibility, which relates the fluid accumulation rate to the pressure rate and couples it with the rate of volume modification:

$$q = \frac{1}{Q}\dot{p} + be \tag{5}$$

  $e = \text{Tr}\, \dot{\boldsymbol{\varepsilon}}$ is the trace of the strain rate tensor, $\mathbf{D}$ is Hooke's tensor of the drained skeleton, b is Biot's coefficient, K is the intrinsic macroscopic permeability and μ_w is the dynamic viscosity of the saturation fluid. Throughout the following sections, the operator $\frac{K}{\mu_w}\mathbf{I}$ will be designated by $\mathbf{H}$. Finally, Q is Biot's modulus.

2 THE LATIN METHOD FOR MULTIPHYSICS PROBLEMS

Recently, a strategy suitable for multiphysics problems was developed based on the LArge Time INcrement method (LATIN) [3]. The LATIN method is a nonincremental iterative approach originally designed for nonlinear time-dependent problems. However, its principles have also been successfully applied to dynamic problems, post-buckling analysis and domain decomposition. (see [4, 5, 6, 7, 8]). For coupled multiphysics problems, the method consists in extending the notion of *material interface* (between substructures) [6] to that of *multiphysics interface*. Such an interface must take into account the coupling between the constitutive relations. To be self-consistent, we only briefly recall in this section the main features of the LATIN strategy for multiphysics problems and the previously obtained results. More details can be found in [9, 10].

At each iteration, the LATIN method produces an approximation of the solution over the whole domain and over the entire time interval being studied. The method is based on three principles:

- **The first principle** consists in separating the difficulties. For coupled field problems, a first set of equations, $\mathbf{A_d}$, containing the so-called admissibility conditions is defined. In order to avoid dealing with both a global and a coupled problem simultaneously, the remaining equations are grouped into a second set of equations, $\mathbf{\Gamma}$; these equations, which are local in the space variables, are the constitutive relations. The solution, i.e. the set of the fields belonging to both $\mathbf{A_d}$ and $\mathbf{\Gamma}$, is found using an iterative procedure.

- **The second principle** of the method consists in using search directions to build approximate solutions of $\mathbf{A_d}$ and $\mathbf{\Gamma}$ alternatively until a sufficient convergence level has been reached (see **Figure 1**).

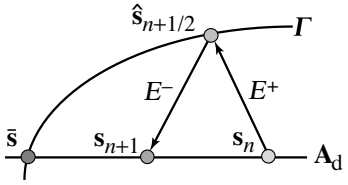

Figure 1: 2-stage LATIN iteration number $n+1$

Each iteration consists of 2 stages: once an element $\mathbf{s}_n \in \mathbf{A_d}$ is known, the *local stage* of iteration $n+1$ uses an initial search direction E^+ to provide an element $\hat{\mathbf{s}}_{n+1/2} \in \mathbf{\Gamma}$. We choose the form of the search direction at the local stage as:

$$\begin{aligned} (\hat{\boldsymbol{\sigma}}_{n+1/2} - \boldsymbol{\sigma}_n) + \mathbf{L}(\hat{\dot{\boldsymbol{\varepsilon}}}_{n+1/2} - \dot{\boldsymbol{\varepsilon}}_n) &= 0 \\ (\hat{q}_{n+1/2} - q_n) + r(\hat{p}_{n+1/2} - p_n) &= 0 \\ (\underline{\hat{W}}_{n+1/2} - \underline{W}_n) + \mathbf{H}(\underline{\hat{Z}}_{n+1/2} - \underline{Z}_n) &= 0 \end{aligned} \tag{6}$$

$\mathbf{L}$, r and $\mathbf{H}$ are three parameters of the method; they do not influence the solution once convergence has been reached. However, their values modify the convergence rate of the algorithm.

At each integration point, using the constitutive relations (3,4,5), the local stage leads to the resolution of a small system of ordinary differential equations in the local space variables. This small sized system is linear as long as the constitutive relations are also linear:

$$\begin{aligned} \mathbf{L}\hat{\dot{\boldsymbol{\varepsilon}}}_{n+1/2} + \mathbf{D}\hat{\boldsymbol{\varepsilon}}_{n+1/2} - b\hat{p}_{n+1/2}\mathbf{I} &= \mathbf{A}_n \\ \frac{1}{Q}\hat{\dot{p}}_{n+1/2} + r\hat{p}_{n+1/2} + b\hat{e}_{n+1/2} &= \alpha_n \\ 2\mathbf{H}\underline{\hat{Z}}_{n+1/2} &= \underline{\beta}_n \end{aligned} \tag{7}$$

where $\mathbf{A}_n = \boldsymbol{\sigma}_n + \mathbf{L}\dot{\boldsymbol{\varepsilon}}_n$, $\alpha_n = q_n + rp_n$ and $\underline{\beta}_n = \underline{W}_n + \mathbf{H}\underline{Z}_n$ are known quantities from local stage $n+1$, and with the initial conditions on the pressure and strain fields.

Once an element $\hat{\mathbf{s}}_{n+1/2} \in \boldsymbol{\Gamma}$ is known, the *linear stage* provides an element $\mathbf{s}_{n+1} \in \mathbf{A_d}$. $\mathbf{s}_{n+1}$, which must satisfy the admissibility relations, is sought along a search direction E^- conjugate of the previous one, so that the mechanical and hydraulic problems remain uncoupled:

$$\begin{aligned}(\boldsymbol{\sigma}_{n+1} - \hat{\boldsymbol{\sigma}}_{n+1/2}) - \mathbf{L}(\dot{\boldsymbol{\varepsilon}}_{n+1} - \hat{\dot{\boldsymbol{\varepsilon}}}_{n+1/2}) &= 0 \\ (q_{n+1} - \hat{q}_{n+1/2}) - r(p_{n+1} - \hat{p}_{n+1/2}) &= 0 \\ (\underline{W}_{n+1} - \underline{\hat{W}}_{n+1/2}) - \mathbf{H}(\underline{Z}_{n+1} - \underline{\hat{Z}}_{n+1/2}) &= 0\end{aligned} \tag{8}$$

One can note that the search directions in linear stage n and local stage $n+1$ are conjugates if the parameters of these directions are kept constant.

In order to use a finite element approach, the admissibility of $\mathbf{s}_{n+1}$ is expressed using a variational formulation. On the one hand, this admissibility condition consists in $\underline{U} \in \mathcal{U}^{[0,T]}$ and $\boldsymbol{\sigma} \in \mathcal{S}^{[0,T]}$ such that:

$$\forall t \in [0,T], \quad \forall \underline{U^\star} \in \mathcal{U}_0, \int_\Omega \mathrm{Tr}[\boldsymbol{\sigma}\boldsymbol{\varepsilon}(\underline{U^\star})]d\Omega = \int_{\partial_2\Omega} \underline{F_d} \cdot \underline{U^\star} dS \tag{9}$$

where $\mathcal{U}_0$ is the set of the finite-energy displacement fields on Ω which vanish on $\partial_1\Omega$. On the other hand, the admissibility condition also consists in $p \in \mathcal{P}^{[0,T]}$, $q \in \mathcal{Q}^{[0,T]}$ and $\underline{W} \in \mathcal{W}^{[0,T]}$ such that:

$$\forall t \in [0,T], \quad \forall p^\star \in \mathcal{P}_0, \int_\Omega (qp^\star + \underline{W} \cdot \underline{\mathrm{grad}}\, p^\star)d\Omega = \int_{\partial_4\Omega} w_d p^\star dS \tag{10}$$

where $\mathcal{P}_0$ is the set of the finite-energy pressure fields on Ω which vanish on $\partial_3\Omega$. Equations (9) and (10) define two uncoupled global problems parameterized by time t.

The convergence of this approach is proved for the case where $\mathbf{L}$, r and $\mathbf{H}$ are positive definite operators which remain constant throughout the iterations [3].

- **The third principle** uses the fact that the successive approximations are defined over both the entire domain and the entire time interval to represent the solution on a radial loading basis. This last point was detailed in [3] and developed, for this particular case, in [9, 10]. Briefly, this approach enables one to reduce the number of space fields generated and, therefore, the number of global systems to be solved. This point will not be developed herein.

Using the third principle, [10] exemplified the competitivity of the method when compared to a classical partitioning incremental strategy: the ISPP method [11]. Moreover, the proposed approach is modular as it allows independent descriptions of the solution fields for each physics, all the coupling being recovered at the local stage. In [10], this modularity was used to define a multi-time-scale strategy. This strategy enables one to use different time steps for the solid and fluid parts of the problem. In particular, in order to perform an iso-quality simulation (i.e. with identical contributions to the global error) the fluid part requires a smaller time step than the solid.

3 A NONLINEAR BEHAVIOR

Most of the consolidation problems which have been analyzed so far are limited to the assumption of linear elastic constitutive behavior and constant permeability, but in most geotechnical situations the behavior of the soil is nonlinear. Following Kondner and his co-workers [12], the stress-strain curves for both clay and sand in a conventional triaxial compression test (constant σ_3) may be approximated by a hyperbolic equation of the form:

$$\sigma_1 - \sigma_3 = \frac{\varepsilon_1}{A + B\varepsilon_1} \tag{11}$$

which relates the difference between the major principal stress σ_1 and the minor principal stress σ_3 to the major principal strain ε_1. A and B are material constants which can be determined experimentally. Then, Hooke's law is defined by:

$$\boldsymbol{\sigma} = \mathbf{D}(\boldsymbol{\varepsilon})\boldsymbol{\varepsilon} - bp\mathbf{I} \tag{12}$$

However, Kondner's model (11) is available only for one-dimensional analysis. This is the case of the following numerical test. There is also evidence that the intrinsic permeability is not constant, even in the case of full saturation. It seems reasonable [1] to assume a dependency of the permeability on the void ratio (or porosity) as well as on the deformation. We propose to test the LATIN method on a variation of one of the laws given in [13] for the intrinsic permeability:

$$K(\boldsymbol{\varepsilon}) = K_0 \frac{n_0}{1+n_0}\left(1 + \frac{1}{n_0}\left\langle \frac{\operatorname{Tr}\boldsymbol{\varepsilon} - \operatorname{Tr}\boldsymbol{\varepsilon}_0}{-\operatorname{Tr}\boldsymbol{\varepsilon}_0}\right\rangle_+^{\alpha}\right) \tag{13}$$

where $\langle\cdot\rangle_+$ denotes the positive part, K_0 and n_0 the initial intrinsic permeability and porosity, $\boldsymbol{\varepsilon}_0$ the strain below which the intrinsic permeability cannot decrease (typically $\operatorname{Tr}\boldsymbol{\varepsilon}_0 = -n_0$), and α a material constant. Darcy's law is then defined by:

$$\underline{W} = \mathbf{H}(\boldsymbol{\varepsilon})\underline{Z} \tag{14}$$

Thus, the consolidation problem which is to be simulated is nonlinear. For 3D extensions of the nonlinear model, one can refer, for instance, to [14].

3.1 Choice of search directions of the LATIN

The search direction E^+ at the local stage (6) is transformed into:

$$\begin{aligned}(\hat{\boldsymbol{\sigma}}_{n+1/2}-\boldsymbol{\sigma}_n)+\mathbf{L}_{n-1/2}(\hat{\dot{\boldsymbol{\varepsilon}}}_{n+1/2}-\dot{\boldsymbol{\varepsilon}}_n)=0\\ (\hat{q}_{n+1/2}-q_n)+r(\hat{p}_{n+1/2}-p_n)=0\\ (\underline{\hat{W}}_{n+1/2}-\underline{W}_n)+\mathbf{H}_{n-1/2}(\underline{\hat{Z}}_{n+1/2}-\underline{Z}_n)=0\end{aligned} \tag{15}$$

and the conjugated search direction E^- at the linear stage (8) into:

$$\begin{aligned}(\boldsymbol{\sigma}_{n+1}-\hat{\boldsymbol{\sigma}}_{n+1/2})-\mathbf{L}_{n+1/2}(\dot{\boldsymbol{\varepsilon}}_{n+1}-\hat{\dot{\boldsymbol{\varepsilon}}}_{n+1/2})=0\\ (q_{n+1}-\hat{q}_{n+1/2})-r(p_{n+1}-\hat{p}_{n+1/2})=0\\ (\underline{W}_{n+1}-\underline{\hat{W}}_{n+1/2})-\mathbf{H}_{n+1/2}(\underline{Z}_{n+1}-\underline{\hat{Z}}_{n+1/2})=0\end{aligned} \tag{16}$$

$\mathbf{L}_{n+1/2}$, r and $\mathbf{H}_{n+1/2}$ are three parameters of the method. The system (7) to be solved at the local stage is then re-written as:

$$\begin{aligned}\mathbf{L}_{n-1/2}\hat{\dot{\boldsymbol{\varepsilon}}}_{n+1/2}+\mathbf{D}(\hat{\boldsymbol{\varepsilon}}_{n+1/2})\hat{\boldsymbol{\varepsilon}}_{n+1/2}-b\hat{p}_{n+1/2}\mathbf{I}=\mathbf{A}_n\\ \frac{1}{Q}\hat{\dot{p}}_{n+1/2}+r\hat{p}_{n+1/2}+b\hat{e}_{n+1/2}=\alpha_n\\ (\mathbf{H}_{n-1/2}+\mathbf{H}(\hat{\boldsymbol{\varepsilon}}_{n+1/2}))\underline{\hat{Z}}_{n+1/2}=\underline{\beta}_n\end{aligned} \tag{17}$$

This nonlinear system (17) is solved using a Newton-type scheme.

Many choices of $(\mathbf{L}_{n+1/2}, r, \mathbf{H}_{n+1/2})$, all of which ensure the convergence of the LATIN method, are available [3]. The easiest way is to take a constant search direction. In dimensional analysis, r can be chosen in the form $r=\frac{1}{Qt_h}$, where t_h is an arbitrary characteristic time, and $(\mathbf{L}_{n+1/2}, \mathbf{H}_{n+1/2})$:

$$\forall n,\quad \mathbf{L}_{n+1/2}=t_m\mathbf{D}(\hat{\boldsymbol{\varepsilon}}=\mathbb{O})\quad\text{and}\quad \mathbf{H}_{n+1/2}=\mathbf{H}(\hat{\boldsymbol{\varepsilon}}=\mathbb{O})=\frac{K_0}{\mu_w}\mathbf{I} \tag{18}$$

where t_m is an arbitrary characteristic time. This choice allows one to assemble operators $\mathbf{L}_{n+1/2}$ and $\mathbf{H}_{n+1/2}$ only once at the beginning of the algorithm. In [3], it was shown that optimal convergence of the method can require the update of the search direction. In the present case of a multiphysics problem, we consider:

$$\begin{aligned}(\boldsymbol{\sigma}_{n+1}-\hat{\boldsymbol{\sigma}}_{n+1/2})-t_m\mathbf{D}(\hat{\boldsymbol{\varepsilon}}_{n+1/2})(\dot{\boldsymbol{\varepsilon}}_{n+1}-\hat{\dot{\boldsymbol{\varepsilon}}}_{n+1/2})=0\\ (q_{n+1}-\hat{q}_{n+1/2})-r(p_{n+1}-\hat{p}_{n+1/2})=0\\ (\underline{W}_{n+1}-\underline{\hat{W}}_{n+1/2})-\mathbf{H}(\hat{\boldsymbol{\varepsilon}}_{n+1/2})(\underline{Z}_{n+1}-\underline{\hat{Z}}_{n+1/2})=0\end{aligned} \tag{19}$$

which is equivalent to:

$$\begin{aligned}\mathbf{L}_{n+1/2}(t)=t_m\mathbf{D}(\hat{\boldsymbol{\varepsilon}}_{n+1/2}(t))\\ \mathbf{H}_{n+1/2}(t)=\mathbf{H}(\hat{\boldsymbol{\varepsilon}}_{n+1/2}(t))\end{aligned} \tag{20}$$

Such a choice requires the assembly and factorization of the operators not only at each iteration, but also at each time step. A new approximation consists in defining an average of the operators over the time interval $[0, T]$:

$$\begin{aligned} \mathbf{L}_{n+1/2} &= \frac{1}{T}\int_{[0,T]} t_m \mathbf{D}(\hat{\boldsymbol{\varepsilon}}_{n+1/2}(t))dt \\ \mathbf{H}_{n+1/2} &= \frac{1}{T}\int_{[0,T]} \mathbf{H}(\hat{\boldsymbol{\varepsilon}}_{n+1/2}(t))dt \end{aligned} \tag{21}$$

Another option would be to define piecewise constant operators.

3.2 Numerical results

The proposed test case concerns the consolidation of a Berea sandstone soil. The material characteristics in **Table 1** were identified in [15]. The geometry is shown in **Figure 2**. The simulation was performed for the one-dimensional case, since the law (11) is defined only in that case.

Initial porosity	$n_0 = 0.19$	Initial Young's modulus	$E_0 = 14.4$ GPa
Poisson's coeff.	$\nu = 0.2$	Biot's modulus	$Q = 13.5$ GPa
Biot's coeff.	$b = 0.78$	Initial permeability	$\frac{K_0}{\mu_w} = 2\ 10^{-10}$ m^3.s.kg^{-1}

Table 1: Characteristics of a water-saturated Berea sandstone poroelastic material

The time interval was $T = 1$ s with $t_1 = T/2$ and the pressures were $p_1 = 10$ MPa and $p_0 = 0.1$ MPa; the initial condition were $p(t = 0) = p_0$; the height of the structure was $L = 5$ m, discretized into 100 elements (quadratic interpolation for displacements and linear interpolation for pore pressures). The search direction parameters were set to $t_m = 9\ 10^{-3}\ t_c$ and $t_h = 8\ 10^{-3}\ t_c$, where $t_c = 9.3$ s.

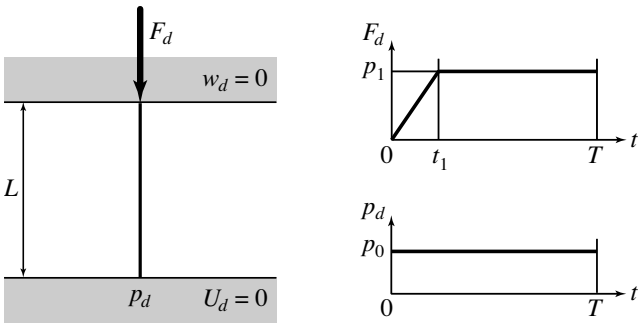

Figure 2: The 1D force-driven test problem

Two simulations were performed to illustrate the behavior of the method when non-linearity increases. The first test was dedicated to the evaluation of the influence of

stiffness: in (11), the value of A and σ_3 were set to $A = \frac{1}{E_0}$ and $\sigma_3 = 0$ while the value of B increased from 0 (which corresponds to the linear case) to 1 GPa^{-1}. The second test concerned the evaluation of the influence of permeability: in (13), the value of α was set to $\alpha = 3$ while the initial porosity $n_0 = -\operatorname{Tr} \boldsymbol{\varepsilon}_0$ was no longer that of the Berea sandstone, but was assumed to decrease from 0.9 to 0.01. (The linear case was recovered by taking $n_0 \to +\infty$.)

From here on, the error indicator based on the difference between an element $\mathbf{s}$ of $\mathbf{A_d}$ and an element $\hat{\mathbf{s}}$ of $\boldsymbol{\Gamma}$ will be used:

$$\hat{\eta} = \frac{e(\hat{\mathbf{s}} - \mathbf{s})}{\frac{1}{2} e(\hat{\mathbf{s}} + \mathbf{s})} \tag{22}$$

with

$$e^2(\hat{\mathbf{s}} - \mathbf{s}) = \|e_t(\hat{\mathbf{s}} - \mathbf{s})\|_T^2 \qquad e_t^2(\hat{\mathbf{s}} - \mathbf{s}) = \frac{1}{2}\|\hat{\boldsymbol{\varepsilon}} - \boldsymbol{\varepsilon}\|_{\mathbf{D}}^2 + \frac{1}{2}\|\hat{p} - p\|_{Q^{-1}}^2$$

and

$$\|\boldsymbol{\varepsilon}\|_{\mathbf{D}}^2 = \int_\Omega \operatorname{Tr}[\boldsymbol{\varepsilon}\mathbf{D}(\hat{\boldsymbol{\varepsilon}} = \mathbb{O})\boldsymbol{\varepsilon}] d\Omega \quad \|p\|_{Q^{-1}}^2 = \int_\Omega p Q^{-1} p d\Omega \quad \|\alpha\|_T^2 = \int_{[0,T]} \alpha^2 dt$$

Figure 3(a) and **Figure 4(a)** show that if constant search directions, such as (18), are used (as in [9, 10]) the convergence rate is very dependent on the degree of nonlinearity. One can see in **Figure 3(b)** and **Figure 4(b)** that if updated average search directions, such as (21), are used at each iteration the convergence rate becomes nearly independent of the degree of nonlinearity. In that case, even if the number of iterations is smaller, the strategy could become very expensive because it requires the assembly and factorization of the operators at each iteration. However, one can note that nearly identical results can be obtained by using updated search directions only during the first iterations (usually 4 or 5). This reduces the computational cost significantly. Let us observe that nonlinearities do not increase the number of iterations needed to reach a given error.

4 A SPATIAL MULTISCALE APPROACH

In this section, we propose to go further in using the modularity of the approach. We are interested in taking into account meshes that can be different for each physics. This will be the case, for instance, if each solver module can provide adaptivity by generating its own finite element mesh.

Following the approach used in [10] for multi-time-scale strategy, the information exchange between the two physics has only to be performed at local stage, the linear stages remaining unchanged.

In this section, we will test the feasibility of such an approach for a 2D linear poroelasticity case, the extension to nonlinear case does not raise any difficulty.

Contrary to previous works on spatial multiscale approach for LATIN method [6, 7], no scale is embedded into the other: the two meshes can be completely independent.

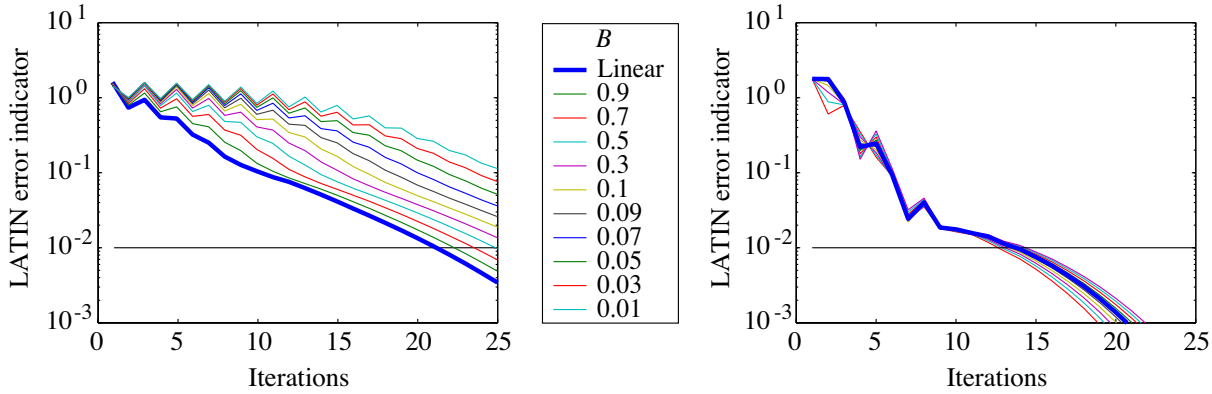

(a) Constant search direction **(b)** Variable search direction

Figure 3: Convergence rates

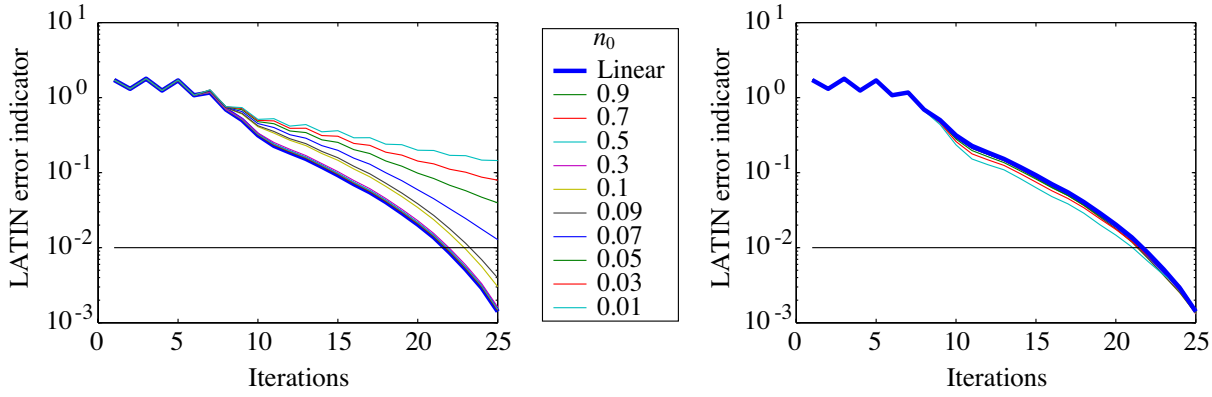

(a) Constant search direction **(b)** Variable search direction

Figure 4: Convergence rates

Therefore, a specific procedure must be developed. The last particularity is that the coupling is performed at local stage and in such a case, the information to be exchanged between the two meshes is stored at integration points of each mesh. The description of the following test case will illustrate the situation.

4.1 2D test case

The proposed test case still concerns the consolidation of a Berea sandstone soil but the simulation was performed in the two-dimensional case. The same material characteristics as in **Table 1** were used and the behavior was assumed to be linear. The geometry is shown in **Figure 5**. The time interval was $T = 36$ s, with $t_1 = T/10$ and the pressures were $p_1 = 1.54$ GPa and $p_0 = 380$ MPa; the initial condition were $p(t = 0) = p_0$.

Figure 6 shows the two independent meshes that were used to describe the solid and

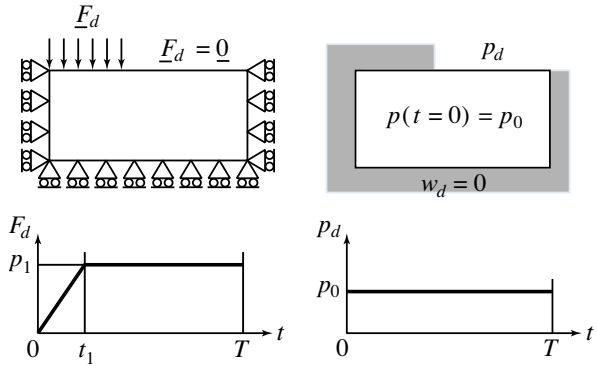

Figure 5: The 2D force-driven test problem

the fluid fields.

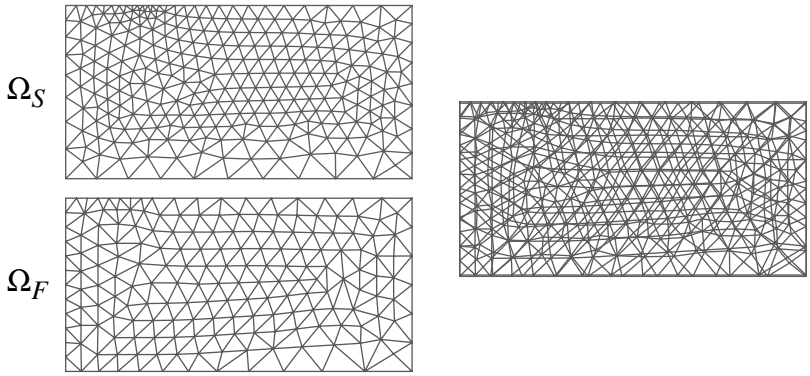

Figure 6: Solid and fluid meshes

4.2 Principles of information transfert

If we consider the constitutive relations (3,4,5), the solid fields being defined on mesh Ω_S and the fluid fields on mesh Ω_F, one needs two dual information transfer operators $\mathcal{P}_{FS}$ and $\mathcal{P}_{SF}$ projecting fields from Ω_S to Ω_F and conversely, in order to re-state the local stage (7) as:

$$\mathbf{L}\hat{\dot{\boldsymbol{\varepsilon}}}_{n+1/2} + \mathbf{D}\hat{\boldsymbol{\varepsilon}}_{n+1/2} = \mathbf{A}_n + b(\mathcal{P}_{SF}\hat{p}_{n+1/2})\mathbf{I} \tag{23}$$

$$\frac{1}{Q}\hat{\dot{p}}_{n+1/2} + r\hat{p}_{n+1/2} = \alpha_n - b(\mathcal{P}_{FS}\hat{e}_{n+1/2}) \tag{24}$$

$$2\mathbf{H}\hat{\underline{Z}}_{n+1/2} = \underline{\beta}_n \tag{25}$$

This new local stage can then be solved, as for the multi-time-scale method, with a fixed point between (23) and (24). Practically, only 3 or 4 iterations are required.

Let us first consider a space field $e_S(\underline{M})$ defined on Ω_S. Following the framework used for different time scales, the projection $e_F(\underline{M}) = \mathcal{P}_{FS} e_S(\underline{M})$ is defined as a generalized average extraction on the basis generated by fonctions φ_F^i (cf. **Figure 7**):

$$\forall i, \quad \int_{\Omega_F} \varphi_F^i \cdot e_F d\Omega_F = \int_{\Omega_S} \varphi_F^i \cdot e_S d\Omega_S \tag{26}$$

Several choices are possible for basis functions and will be discussed in the next sections.

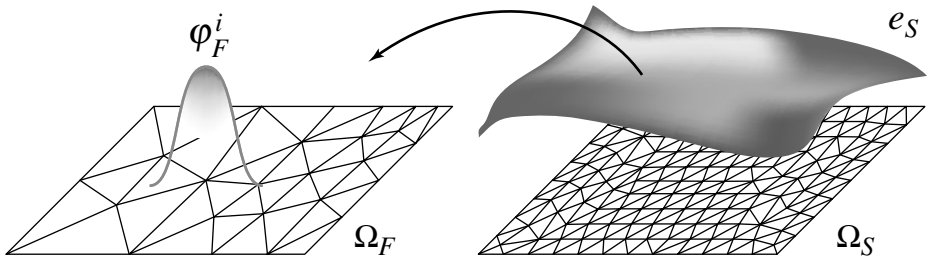

Figure 7: A generalized average extraction

4.3 Case of C^0 nodal fields

If e_S and e_F are nodal fields (continuous on the whole meshes Ω_S and Ω_F), one can use diffuse approximation weighting functions [16], finite element shape functions, etc. As a first step, we propose herein to use this last choice. For continuous fields over the meshes, if N_S, N_F store the finite element shape functions of each meshes and E_S, E_F the nodal values of the fields:

$$\begin{aligned} e_S &= N_S E_S \\ e_F &= N_F E_F \end{aligned} \tag{27}$$

then one gets:

$$\int_{\Omega_F} N_F^T N_F E_F d\Omega_F = \int_{\Omega_S} N_F^T N_S E_S d\Omega_S \tag{28}$$

or $M_{FF} E_F = M_{SF}^T E_S$ where M_{FF} is the classical cross product of shape functions on Ω_F and $M_{SF} = \int_{\Omega_S} N_S^T N_F d\Omega_S$ is computed with a specific technique, for instance the one in [17]. In this case, $E_F = M_{FF}^{-1} M_{SF}^T E_S$ and one recovers Mortar projection method with classical shape functions [18]. The main drawback is the costly use of M_{FF}^{-1} (global matrix on the whole mesh).

4.4 Suited method for multiphysics problems

For the case we are interested into, the various fields are evaluated at integration points of Ω_S for the volumic strain e_S and of Ω_F for the pore pressure p_F and do not possess C^0 regularity.

A suited projection consists in using as test functions the restriction of each finite element shape functions for a given element. They are non longer continuous throughout the elements, the projection will not give continuous functions (which is not mandatory in our case), but will localize the computations on each element (cf. **Figure 8**).

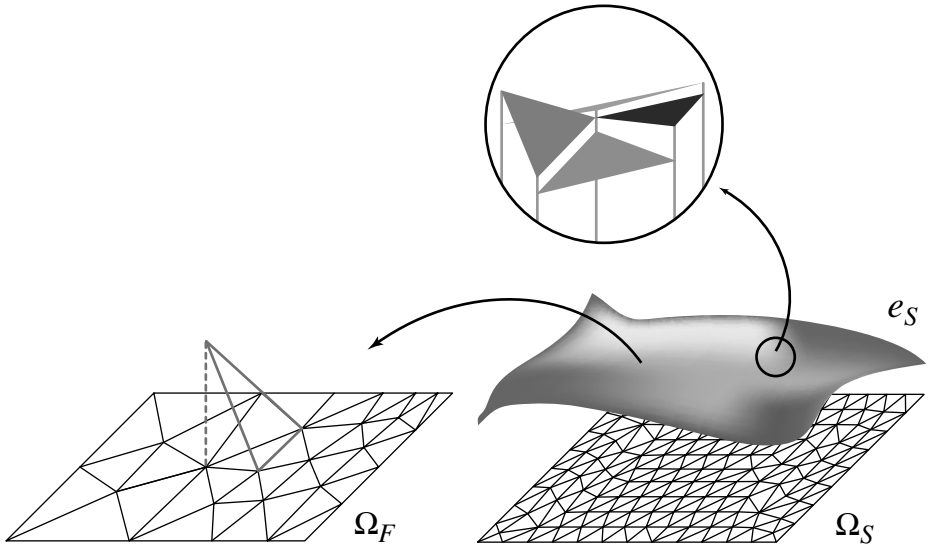

Figure 8: A generalized average extraction for non continuous fields

The procedure to get $e_F = \mathcal{P}_{FS} e_S$ is therefore the following:

- the values of e_S at integration points of an element of Ω_S are extrapolated to the nodes of the same element (for instance using shape functions of Ω_S);
- the resulting elementary field is projected onto an element of Ω_F using *local* elementary matrices M_{FF}^{-1} and M_{SF}^{T};
- the contributions are summed on the elements independently;
- the resulting field is interpolated at integration points of Ω_F (using shape functions of Ω_F) element per element, to get e_F.

Main properties are:

- the reciprocal projection from Ω_F to Ω_S is defined with duality, conserving the energy:

$$\int_{\Omega_F} e_F p_F d\Omega_F = \int_{\Omega_S} e_S p_S d\Omega_S \tag{29}$$

  for any field e_S. One gets the transposed of operator $\mathcal{P}_{FS}$, with respect to the previous energy symmetric form (29), as the projection $\mathcal{P}_{SF}$;

- the fomulation is symmetric, i.e. one gets the above defined $\mathcal{P}_{SF}$ operator with similar operations as for $\mathcal{P}_{FS}$, using M_{SS}^{-1} and M_{SF} elementary matrices;
- both projections $\mathcal{P}_{SF}$ and $\mathcal{P}_{FS}$ satisfy to the patch-test (i.e. perfect projection of any field that can be represented on both meshes Ω_S and Ω_F).

4.5 Numerical results

Figure 9 compares the evolution of the maximum pore pressure over the time interval $[0, T]$ when the multi-space-scale and the mono-space-scale (cf. [9]) on a refined mesh to get a reference solution. One can see that the results are very similar.

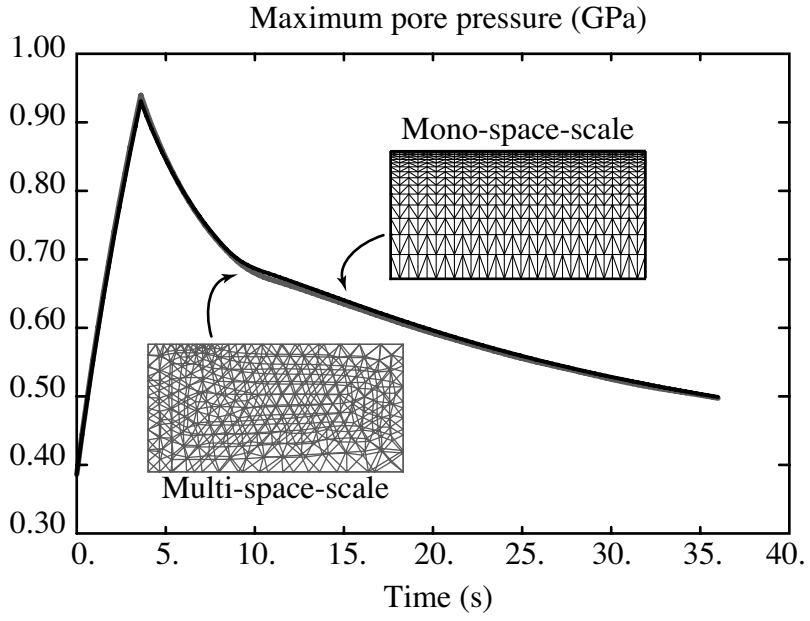

Figure 9: Comparison of the maximum pore pressure

The solution at convergence of the multi-space-scale strategy verifies the following equations:

$$\boldsymbol{\sigma} = \mathbf{D}\boldsymbol{\varepsilon} - b(\mathcal{P}_{SF}p)\mathbf{I}, \quad q = \frac{1}{Q}\dot{p} + b(\mathcal{P}_{FS}e) \quad \text{and} \quad \underline{W} = \mathbf{H}\underline{Z} \tag{30}$$

as well as the admissibility conditions (9,10). These equations lead to the kinematic formulation of the 2-field problem with the displacement field $\underline{U} \in \mathcal{U}^{[0,T]}$ and the pressure field $p \in \mathcal{P}^{[0,T]}$ as unknowns: $\forall t \in [0,T], \forall \underline{U}^\star \in \mathcal{U}_0, \forall p^\star \in \mathcal{P}_0$,

$$\begin{aligned} \int_{\Omega_S} \mathrm{Tr}[\boldsymbol{\varepsilon}(\underline{U})\mathbf{D}\boldsymbol{\varepsilon}(\underline{U}^\star)]d\Omega_S - \int_{\Omega_S} b(\mathcal{P}_{SF}p)\,\mathrm{Tr}\,\boldsymbol{\varepsilon}(\underline{U}^\star)d\Omega_S &= \int_{\partial_2\Omega_S} \underline{F}_d \cdot \underline{U}^\star dS_S \\ \int_{\Omega_F} \underline{\mathrm{grad}}\, p \cdot \mathbf{H}\, \underline{\mathrm{grad}}\, p^\star d\Omega_F + \int_{\Omega_F} \dot{p}\frac{1}{Q}p^\star d\Omega_F + \int_{\Omega_F} bp^\star(\mathcal{P}_{FS}e)d\Omega_F &= \int_{\partial_4\Omega_F} w_d p^\star dS_F \end{aligned} \tag{31}$$

Using the previous space discretizations, this leads to the coupled global system of equations at each time step:

$$\begin{aligned} KU - A_{SF}p &= f_d \\ Hp + S\dot{p} + A_{FS}\dot{U} &= g_d \end{aligned} \tag{32}$$

K, H and S are the stiffness, permeability and compressibility matrices; f_d are the generalized forces corresponding to $\underline{F}_d$ and g_d is the generalized flux corresponding to w_d. When using identical time discretization for fluid and solid, let us notice that the coupling terms A_{SF} and A_{FS} verify:

$$A_{SF} = A_{FS}^T \tag{33}$$

In the case where identical meshes Ω_S and Ω_F, one recovers the classical monolithic formulation recalled in [9]. By derivating the first group of equations with respect to time, one gets:

$$\begin{bmatrix} K & -A_{SF} \\ -A_{FS} & -S \end{bmatrix} \begin{bmatrix} \dot{U} \\ \dot{p} \end{bmatrix} + \begin{bmatrix} 0 & 0 \\ 0 & -H \end{bmatrix} \begin{bmatrix} U \\ p \end{bmatrix} = \begin{bmatrix} \dot{f}_d \\ -g_d \end{bmatrix} \tag{34}$$

The direct resolution of this system would be very expensive as A_{SF} and A_{FS} are dense matrices.

5 CONCLUSIONS

In this paper, we described a partitioned strategy based on the LATIN approach which enables one to take into account some of the classical nonlinearities of consolidation problems. The numerical tests showed that if updated search directions are used during the first iterations, the convergence rate is nearly independent of the level of nonlinearity. Thus, these nonlinear phenomena do not result in a significant increase in the computational costs.

The modularity of the method was also improved to deal with independent meshes for each physics. The next step will be to mix time and space multiscale features for the physics to be as independent as possible.

REFERENCES

[1] R. W. Lewis and B. A. Schrefler. *The Finite Element Method in the Static and Dynamic Deformation and Consolidation of Porous Media*. Wiley, 2nd edition, 1998.

[2] O. Coussy. *Mechanics of porous continua*. John Wiley & Sons, 1995.

[3] P. Ladevèze. *Nonlinear Computational Structural Mechanics — New Approaches and Non-Incremental Methods of Calculation*. Springer Verlag, 1999.

[4] P. A. Boucard, P. Ladevèze, and H. Lemoussu. A modular approach to 3-D impact computation with frictional contact. *Computer and Structures*, 78/1-3:45–52, 2000.

[5] H. Lemoussu, P. A. Boucard, and P. Ladevèze. A 3-D shock computational strategy for real assembly and shock attenuator. *Advances in Engineering Software*, 33/7-10:517–526, 2002.

[6] P. Ladevèze, O. Loiseau, and D. Dureisseix. A micro-macro and parallel computational strategy for highly heterogeneous structures. *International Journal for Numerical Methods in Engineering*, 52(1–2):121–138, 2001.

[7] P. Ladevèze and A. Nouy. A multiscale computational method with time and space homogenization. *Comptes Rendus Mécanique*, 330:683–689, 2002.

[8] P. Ladevèze, A. Nouy, and O. Loiseau. A multiscale computational approach for contact problems. *Computer Methods in Applied Mechanics and Engineering*, 191:4869–4891, 2002.

[9] D. Dureisseix, P. Ladevèze, and B. A. Schrefler. A computational strategy for multiphysics problems — application to poroelasticity. *International Journal for Numerical Methods in Engineering*, 56(10):1489–1510, 2003.

[10] D. Dureisseix, P. Ladevèze, D. Néron, and B. A. Schrefler. A multi-time-scale strategy for multiphysics problems: application to poroelasticity. To appear in *International Journal for Multiscale Computational Engineering*, 2004.

[11] R. Matteazzi, B. Schrefler, and R. Vitaliani. *Comparisons of partitioned solution procedures for transient coupled problems in sequential and parallel processing*, pages 351–357. Advances in Computational Structures Technology. Civil-Comp Ltd, Edinburgh, Scotland, 1996.

[12] R. L. Kondner. Hyperbolic stress-strain response: cohesive solids. *J. Soil. Mech. Found. Div. ASCE*, 89 (SM1):115–143, 1963.

[13] E. A. Meroi and B. A. Schrefler. Biomechanical multiphase approaches in soft biological tissues. In *Proceedings of the 12th International Conference on Mechanics in Medicine and Biology*, 2002.

[14] L. Dormieux, A. Molinari, and D. Kondo. Micromechanical approach to the behavior of poroelastic materials. *Journal of the Mechanics and Physics of Solids*, 50:2203–2231, 2002.

[15] GRECO. Scientific report, GRECO Géomatériaux, 1990.

[16] P. Villon, H. Borouchaki, and K. Saanouni. Transfert de champs plastiquement admissibles. *Comptes Rendus Mécanique*, 330:313–318, 2002.

[17] M. W. Heinstein and T. A. Laursen. A three dimensional surface-to-surface projection algorithm for non-coincident domains. *Communications in Numerical Methods for Engineering*, 19:421–432, 2003.

[18] C. Bernardi, Y. Maday, and A. T. Patera. A new nonconforming approach to domain decomposition: the mortar element method. In H. Brezzi *et al*, editor, *Nonlinear partial differential equations and their applications*, pages 13–51. Paris, 1994.